Journal of Solid State Chemistry 184 (2011) 52–58

Contents lists available at ScienceDirect

Journal of Solid State Chemistry

journal homepage: www.elsevier.com/locate/jssc

Synthesis and spectral characteristics of $Sr_2Y_8(SiO_4)_6O_2$: Eu polycrystals

M.G. Zuev [a,b,*], A.M. Karpov [b], A.S. Shkvarin [c]

[a] Ural Federal University, 620002 Ekaterinburg, Russia
[b] Institute of Solid State Chemistry, Ural Branch of the Russian Academy of Sciences, 620990 Ekaterinburg, Russia
[c] Institute of Metal Physics, Ural Branch of the Russian Academy of Sciences, 620041 Ekaterinburg, Russia

ARTICLE INFO

Article history:
Received 13 August 2010
Received in revised form
11 October 2010
Accepted 12 October 2010
Available online 27 October 2010

Keywords:
Yttrium silicate
X-ray diffraction
Vibrational spectra
Luminescence
Eu^{2+}
Eu^{3+}
Oxygen vacancies

ABSTRACT

Spectral-luminescent characteristics of $Sr_2Y_8(SiO_4)_6O_2$: Eu powder crystal phosphor with the apatite structure and high-intensity luminescence of Eu^{3+} ions have been studied. The charge state of europium in the samples has been characterized by means of X-ray L_3-adsorption spectroscopy. It was established that Eu^{3+} forms two types of optical centers. Besides, luminescence of Eu^{2+} ions was found. Reduction $Eu^{3+} \rightarrow Eu^{2+}$ was considered, which may be due to $V_{Sr}^{||}$ vacancy formation in the 4*f* crystal lattice position and to negative charge transfer by this vacancy to two Eu_Y^{3+} ions. Thus, in the silicate lattice there exist inhomogeneously distributed oxygen-deficient centers, which are responsible for nonradiative transfer of excitation energy to Eu^{3+} and Eu^{2+} ions. To study electron-vibrational interactions in the crystal phosphor samples, their IR and Raman spectra were examined. In the luminescence spectrum of Eu^{2+}, a series of low-intensity bands caused by interaction of the $4f^6 5d$ state of Eu^{2+} with silicate lattice vibrations was observed.

1. Introduction

Studying of crystal phosphor formation and the nature of their luminescence is an actual problem, which is especially important for designing of new effective luminophor with high-intensity luminescence.

It is interesting to know the influence of doped RE-ions structural defects, on a luminescence. Defects are formed, in particular, when as a RE-ion europium is used. Europium can be in crystal matrixes simultaneously in the form Eu^{3+} and Eu^{2+} ions that lead to formation of oxygen vacancies. In addition europium ions can occupy nonequivalent crystallographic positions in a lattice, forming the various optical centers. The interpretation of a luminescence spectral composition is interested in this case.

At present, the method for obtaining white light is the combination green, red and blue light-emitting phosphors. However red light-emitting phosphors used for white light-emitting diode such as Y_2O_2S: Eu^{3+}, ZnCdS: Cu, Al, has chemical instability and low efficiency of luminescence. Apatite-structure silicates are known as effective matrixes for activation by their RE-ions. Due to high luminescence intensity and chemical stability up to 1000 °C this materials can be used as active laser media and red light-emitting for white light-emitting diode [1–6].

For example in [4] temperature dependence of Eu^{3+} luminescence in $Ca_2Gd_8Si_6O_{26}$ was investigated. This compound is a perspective as thermometric phosphor. In work [5] the photoluminescence of $Ca_2Gd_8(SiO_4)_6O_2$: Dy^{3+} thin film was investigated. This compound can be used for devices with high resolution. Seeta Rama Raju et al. [6] identified two kinds of optical centers in $Ca_2Gd_8Si_6O_{26}$: Eu^{3+} which was formed by Eu^{3+} ions. These materials find a use for optical display.

In this investigation spectral-luminescent characteristics of $Sr_2Y_8(SiO_4)_6O_2$: Eu powder crystal phosphor with the apatite structure and high-intensity luminescence of Eu^{3+} ions have been studied. It is known that owing to electronic conditions Eu^{3+} ion are an optical sensor. On the basis of Eu^{3+} luminescence spectrum studies, the information about the number and the structure of optical centers formed by europium in the crystal lattice was obtained. In addition, we examined the $Eu^{3+} \rightarrow Eu^{2+}$ transition in the crystals, which is due apparently to $V_{Sr}^{||}$ vacancy formation in the 4*f* crystal lattice site and to negative charge transfer by this vacancy to two Eu_Y^{3+} ions. Through spectroscopic method were found oxygen deficient centers which nonradiative transfer the excitation energy to Eu^{3+} and Eu^{2+} ions. The mechanism of centers formation was proposed.

To study electron-vibrational interactions in the crystal phosphor samples, their IR and Raman spectra were examined.

2. Experimental

The samples for analysis were synthesized by two-stage calcination of a mixture of raw materials in air. At the first stage we used

* Corresponding author.
E-mail address: zuev@ihim.uran.ru (M.G. Zuev).

0022-4596/$ - see front matter © 2010 Elsevier Inc. All rights reserved.
doi:10.1016/j.jssc.2010.10.014

$SrCO_3$, Y_2O_3, Eu_2O_3, SiO_2 reagents (all 99.99% pure) and the synthesized compounds $Sr_2Y_8Si_6O_{26}$ and $Sr_2Eu_8Si_6O_{26}$ as raw materials. Stoichiometric amounts of the initial components were carefully mixed in an agate mortar with addition of ethanol. Then the powders were placed in alundum crucibles and calcined in air in the temperature interval 1200–1400 °C for 80 h with intermediate restacking of the mixture. The time of calcination was sufficient to equilibrate the system [2]. At the second stage, an activator was used. Stoichiometric amounts of $Sr_2Y_8Si_6O_{26}$ and $Sr_2Eu_8Si_6O_{26}$ were combined to obtain solid solutions $Sr_2Y_{8(1-x)}Eu_{8x}Si_6O_{26}$. The agents were carefully mixed, placed in alundum crucibles and calcined in air at temperature 1350–1450 °C for 40 h.

X-ray powder diffraction (DRON-2, Cuk_λ=1.5406) was used to identify the structure of the phosphors [7]. The diffraction patterns of the synthesized solid solutions were processed by Rietveld method with the use of the ICDD card-file.

The charge state of europium in the samples was defined by X-ray L_3-absorption spectroscopy on an ARS-KD-2 X-ray spectrometer. The measurements precision was ±3%.

The IR-spectrum was measured by a Spectrum spectrophotometer (Perkin-Elmer) on powders suspended in vaseline oil in the frequency range 400–1000 cm^{-1}. The Raman-spectrum was measured on a Renishaw spectrometer ($\Delta\nu$=1000 cm^{-1}) using an argon laser (λ=514.5 nm) as an excitation source. The homogeneity region of the solid solutions was defined by X-ray and vibrational spectroscopy.

Photoluminescence and excitation spectra were recorded at room temperature on a grating monochromator MDR-204 (deuterium lamp, Hamamatsu R928 photomultiplier) and a Cary Eclipse Fluorescence Spectrophotometer (Xe pulse lamp with exceptionally long lifetime, pulsed at 80 Hz, pulse width at half peak height ~2 μs, peak power equivalent to 75 kW).

3. Results and discussion

$Sr_2Y_8Si_6O_{26}$ crystals are isostructural to $Sr_2La_8Si_6O_{26}$ [8] having an apatite structure. According to [9], $Sr_2La_8Si_6O_{26}$ crystals (space group $P6_3/m$, Z=1) have the following site-symmetry of atoms: La–4*f*, Sr–4*f*, La–6*h*, Si–6*h*, O–6*h*, O–6*h*, O–12*i*, O–2*a*; Z=1. Since $Sr_2La_8Si_6O_{26}$ and $Sr_2Y_8Si_6O_{26}$ are isomorphous, we assumed that Y atoms also occupy 4*f* and 6*h* sites. Therefore, europium, substituting in $Sr_2Y_8Si_6O_{26}$ for yttrium atoms, may also take these two positions.

Fig. 1 shows an X-ray diffraction pattern of the synthesized solid solutions $Sr_2Y_{8(1-x)}Eu_{8x}Si_6O_{26}$ (x=0.01–0.15). It is seen that all the compounds are formed by the pure apatite phase. The crystal structure of $Sr_2Y_8Si_6O_{26}$ is displayed in Fig. 2.

It is established that as a result of activation of the $Sr_2Y_8Si_6O_{26}$ matrix with europium in $Sr_2Y_8(SiO_4)_6O_2$: Eu samples, Eu^{2+} ions are formed along with Eu^{3+} ions. Fig. 3 demonstrates the quantity of Eu^{2+} ions (%) versus the general concentration (x) of europium in the samples. As is seen, in the interval x=0–0.07 the quantity of Eu^{2+} ions decreases from 42% to 8%, and then remains almost constant.

As Eu^{2+} ions are formed, the chemical formula of the samples can be represented as $Sr_2Y_{8(1-x)}Eu_{8x}Si_6O_{26-\delta}$, where δ is oxygen nonstoichiometry.

The mechanism of Eu^{2+} ion formation is similar to that considered in [10]. As a result of activation of the $Sr_2Y_8Si_6O_{26}$ matrix with europium during high-temperature calcinations,

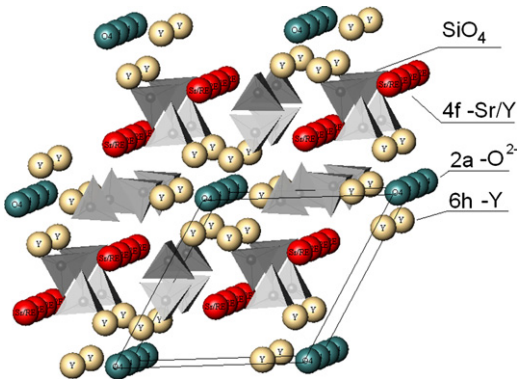

Fig. 2. Crystal structure of $Sr_2Y_8(SiO_4)_6O_2$.

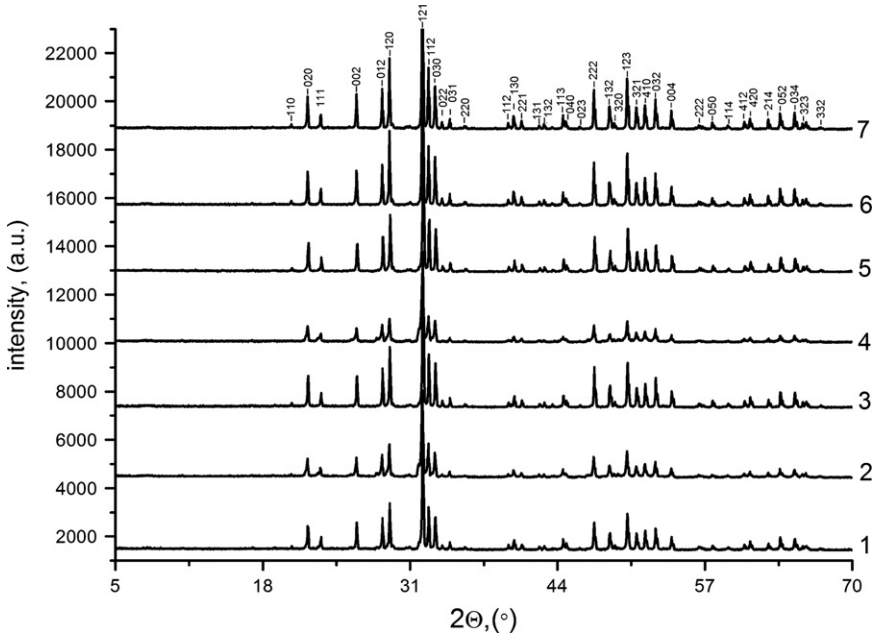

Fig. 1. X-ray diffraction patterns of $Sr_2Y_{8(1-x)}Eu_{8x}(SiO_4)_6O_2$, x=0.01 (1), 0.02 (2), 0.03 (3), 0.05 (4), 0.07 (5), 0.1 (6), 0.15 (7).

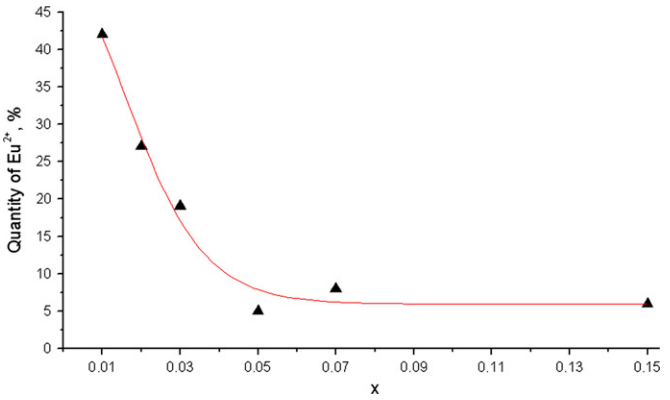

Fig. 3. Dependence of quantity of ions Eu^{2+} from the general concentration of europium in samples.

$V_{Sr}^{\parallel}$ vacancies are formed in the 4*f* site. These defects transfer the negative charge to two Eu_Y^{3+} ions leading to the formation of Eu^{2+} ions and, consequently, of oxygen-deficient centers. Since the quantity of Eu^{2+} decrease in an $x=0.01$–0.07 range, it is possible to conclusion that the number of formed vacancies $V_{Sr}^{\parallel}$ reduces. At $x > 0.07$ the number of vacancies remains to constant.

Fig. 4 shows concentration dependences of lattice parameters *a*, *c* and *V*. When *x* increases, the lattice parameters grow nonlinearly owing to europium → yttrium replacement. It is also visible that the parameter *c* virtually does not change in the interval $x=0-0.03$, while at $x > 0.03$ it increases essentially. It is known [11] that in the apatite structure with space group $P6_3/m$, replacements of ions in the 6*h* position lead to variations in the parameter *a*, whereas replacements in the 4*f* position do not affect this parameter. On the other hand, changes in the parameter *c* depend on replacements in the 4*f* position. Hence, the constant character of the parameter *c* at concentrations $x \leq 0.03$ suggests that yttrium should be replaced by europium primarily in the 6*h* position. At $x > 0.03$ yttrium it is replaced by europium to considerable degree also in the 4*f* position. Therefore, it can be concluded that at $x \leq 0.03 V_{Sr}^{\parallel}$ vacancies transfer a negative charge to two Eu_Y^{3+} ions, which are located in the 6*h* position, where the Eu^{2+} ions are formed. At $x > 0.03$ Eu^{2+} ions can be formed also in the 4*f* position.

In order to refine the structure of optical centers, we examined the crystal lattice dynamics of $Sr_2Y_{8(1-x)}Eu_{8x}Si_6O_{26-\delta}$ phosphors. For this purpose, the factor-group of ideal crystals $Sr_2Y_8Si_6O_{26-\delta}$ vibrations was analyzed. The analysis yielded the following representation of optical vibrations of the silicate:

$$\Gamma_{Sr_2Y_8Si_6O_{26}} = 10A_g(R) + 20E_{1g}(R) + 22E_{2g}(R) + 10A_u(IR) + 20E_{1u}(IR)$$

In the Raman spectrum 52 bands may be expected, and 30 bands—in the IR spectrum. The oscillation spectrum of real $Sr_2Y_{8(1-x)}Eu_{8x}Si_6O_{26-\delta}$ crystals may differ from that of ideal crystals because of defects in the crystal lattice. The influence of europium ions on IR and Raman spectra was considered. Fig. 5 exhibits the IR spectrum of the samples for $x=0$, 0.01, 0.03, 0.05, 0.15, and assignment of some bands in this spectrum is given in Table 1. When europium is introduced into the matrix of $Sr_2Y_8Si_6O_{26-\delta}$, it essentially influences the frequency range corresponding to translation and rotation.

Comparison of frequencies in the IR spectrum of $Sr_2Eu_8Si_6O_{26-\delta}$ with those for the above solid solutions allowed us to assume that frequencies in the range $254-280\ cm^{-1}$ refer to translation and rotation of europium ions. Vibration modes ν_1, ν_2, ν_3, ν_4 of SiO_4 tetrahedra were assigned by analogy [12]. The bands in the frequency range $498.5-517\ cm^{-1}$ can be attributed to bond

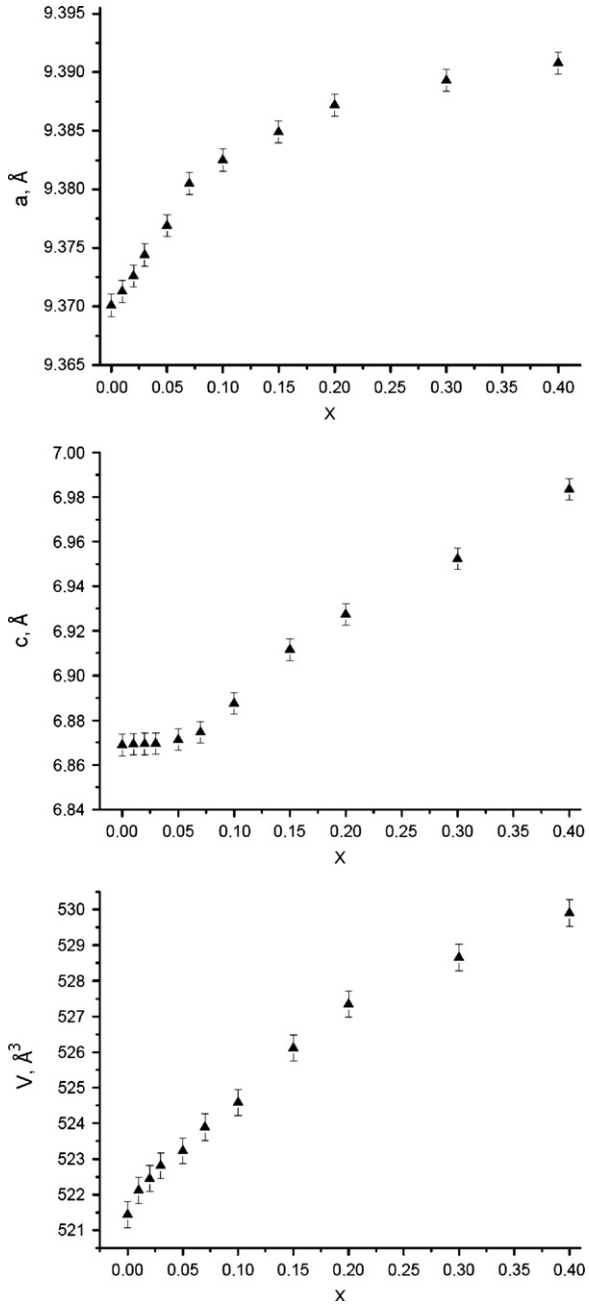

Fig. 4. Concentration dependence of the lattice parameters *a*, *c* and the volume *V* of the solid solution $Sr_2Y_{8(1-x)}Eu_{8x}Si_6O_{26-\delta}$.

vibration of Y(Eu)–O, similarly to assignment of bond vibration frequencies of $Gd-O$ in hydroxyapatite crystals [13].

It is known [14] that vacancies can excite additional frequencies in the vibrational spectrum of crystals. $Sr_2Eu_8Si_6O_{26-\delta}$ has the maximum concentration of oxygen vacancies since it possesses the greatest nonstoichiometry. Therefore, weak bands at 704 and $858\ cm^{-1}$ in these crystals may be due presumably to oxygen vacancies. The bands at 729 ($x=0.02$) and $717\ cm^{-1}$ ($x=0.03$) are also attributed to oxygen vacancies. As x increases from 0.02 to 1, a reduction in frequencies from 729 to $704\ cm^{-1}$ is observed.

Fig. 6 shows the Raman spectrum of two samples $Sr_2Y_{8(1-x)}Eu_{8x}Si_6O_{26-\delta}$ ($x=0$ and 0.1). Inhomogeneously broadened bands are indicative of some disordering in the crystal structure. Frequencies in the spectrum were assigned on the basis of work [15]. The europium ions substituting for yttrium ions are located in the

crystal lattice near to SiO_4 tetrahedra. Therefore, europium is expected to affect the vibrational mode of SiO_4. Indeed, the Raman spectrum of $Sr_2Y_{7.2}Eu_{0.8}Si_6O_{26-\delta}$ (curve 2) contains inactive vibrations (there are no bands) corresponding to frequency modes v_1 and v_2. For other concentrations of europium, such lines are also absent in the Raman spectrum.

Let us now consider the spectral-luminescent characteristics of the samples. Fig. 7 presents the luminescence spectrum of europium in the $Sr_2Y_{6.8}Eu_{1.2}Si_6O_{26-\delta}$ sample ($\lambda_{ex}=400$ nm.) Transitions between 4*f*-levels of Eu^{3+} were noted. A rather high intensity of transitions $^5D_0 \rightarrow {}^7F_2$ shows that Eu^{3+} ions occupy the crystallographic positions which do not coincide with the center of symmetry. The wide band at $\lambda_{max}=443$ nm is due to luminescence of Eu^{2+} ions. In the emission spectrum of Eu^{2+}, small-intensity bands 1–6 are caused by phonon–electron interaction between the state of $4f^65d$ Eu^{2+} ions and the silicate crystal lattice. The wave numbers of these bands are given in Table 2. The difference in the wave numbers (cm^{-1}) is: 1 and 2—937, 2 and 3—323, 3 and 4—748, 4 and 5—375, 5 and 6—749. As follows from analysis of the IR spectrum (Table 1), frequency 937 cm^{-1} can be carried to the v_3 mode of SiO_4, frequency 323 cm^{-1} can be carried to translations and rotations of SiO_4, Y, Sr, and frequencies 748 and 749 cm^{-1}—to vibrations induced by oxygen vacancies. Thus, fluctuations of SiO_4 and oxygen vacancies co-operate with the $4f^65d$ Eu^{2+} ion, which is observed in a series of electron-vibrational transitions from an excited Eu^{2+} state in the ground state.

Fig. 8 shows a part of the emission spectrum for the sample $Sr_2Y_{6.8}Eu_{1.2}Si_6O_{26-\delta}$ excited by light in the interval $\Delta\lambda_{ex}=250-290$ nm. This phosphor has the greatest intensity of luminescence among all solid solutions in this concentration series. The spectra of other samples are similar, with only small shifts in the

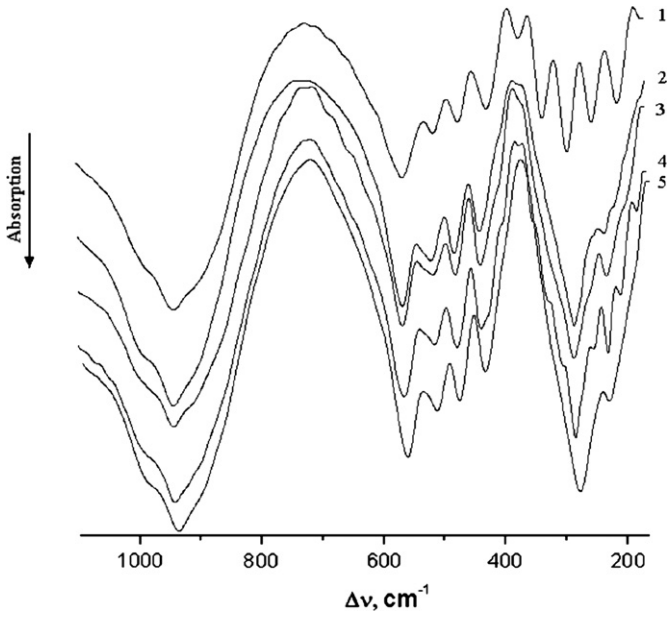

Fig. 5. Infrared absorption spectra of $Sr_2Y_{8(1-x)}Eu_{8x}Si_6O_{26-\delta}$: $x=0(1)$, 0.01(2), 0.03(3), 0.05(4), 0.15(5).

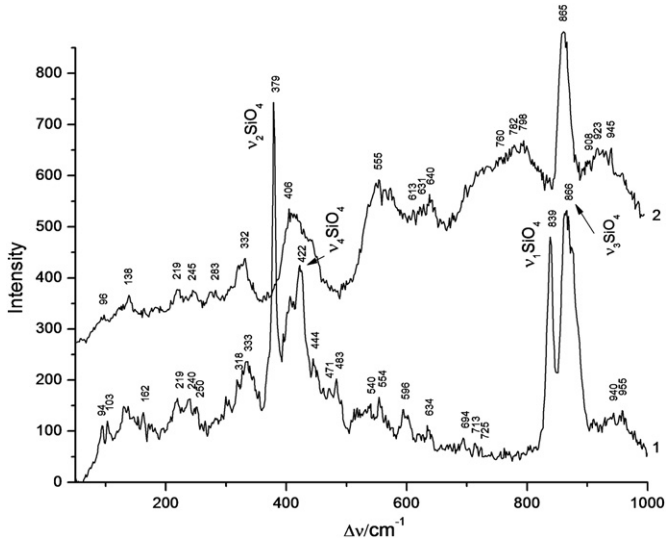

Fig. 6. Raman spectra of $Sr_2Y_{8(1-x)}Eu_{8x}Si_6O_{26-\delta}$: $x=0(1)$, 0.1(2).

Table 1
IR frequencies (cm^{-1}) for the solid solution in $Sr_2Y_{8(1-x)}Eu_{8x}Si_6O_{26-\delta}$.

$x=0$	0.01	0.02	0.03	0.05	0.15	1	Assignment
935	938	935	937	938	937	923	v_3 SiO_4
906 sh*	906 sh	898 sh	904 sh	891 sh	–	892	v_1 SiO_4
–	–	–	–	–	–	858	Oxygen vacancies
–	–	729	717	–	–	704	Oxygen vacancies
–	–	692 sh	682 sh	–	–	–	
–	–	655 sh	655 sh	–	–	–	
560	561	562	561	562	561	551	v_4SiO_4
510	515	517	511.5	512.5	513	498.5	Y(Eu)–O
470	476	476	474	475	476	464	v_2SiO_4
422	435	433	434	435	434	418	
–	–	–	–	424 sh	–	–	
–	401 sh	–	402 sh	403 sh	–	–	
370	373	–	370 sh	372	–	–	
–	–	–	–	351 sh	–	–	Translation and rotation of SiO_4, Y, Sr
331	–	–	314 sh	324 sh	–	322 sh	
290	–	–	–	302 sh	–	276	
–	279	280	280	281	278	254	←Eu
250	–	–	–	251	–	–	
–	230	232	227	227.5	230	–	
–	218 sh	–	–	–	–		
208	–	–	201 sh	207	–	209	
–	–	–	–	180	–	–	

* Shoulder.

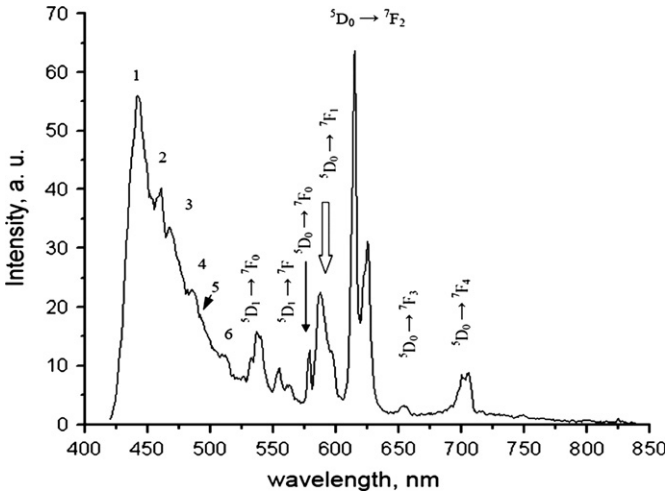

Fig. 7. Luminescence spectrum of $Sr_2Y_{6.8}Eu_{1.2}Si_6O_{26-\delta}$ at excitation λ_{ex}=400 nm.

Table 2
Wave numbers of electron-vibrational transitions in a spectrum of luminescence Eu^{2+} in $Sr_2Y_{6.8}Eu_{1.2}Si_6O_{26-\delta}$.

Number of band	Wave number, cm^{-1}
1	22,626
2	21,689
3	21,366
4	20,618
5	20,243
6	19,494

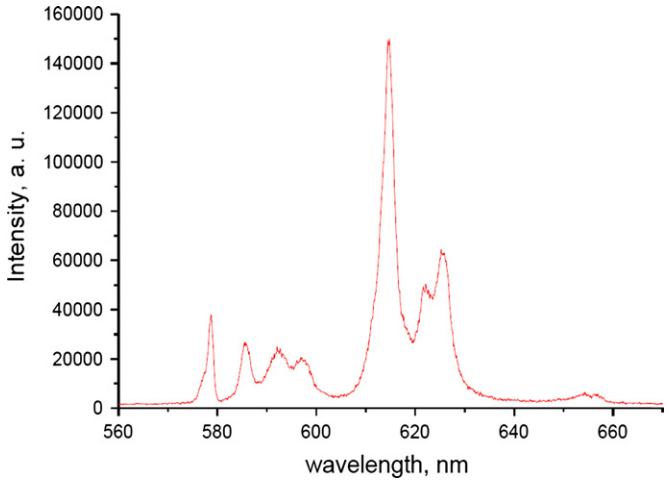

Fig. 8. Fragment of a spectrum of a luminescence of $Sr_2Y_{6.8}Eu_{1.2}Si_6O_{26-\delta}$ at excitation in an interval $\Delta\lambda_{ex}$=250–290 nm.

bands concentration. The transition band $^5D_0 \rightarrow {}^7F_0$ has an inhomogeneous broadening. Its expansion on the Gausslan component allowed us to allocate two bands with peaks at 577 and 581 nm, which confirm the occurrence of two optical centers generated by Eu^{3+}. Splitting of level $^7F_1$ on three Stark sublevels confirms that crystal field symmetry of the ligands forming the optical centers is below of trigonal symmetry [16]. Thus, the spectra presented in Figs. 7 and 8 are total emission spectra of two centers. It is necessary to note, that luminescence spectra of two optical centers is similar. Therefore, the microstructure of a crystal field in system "ion Eu^{3+}+ligands" also is close for these centers. Therefore, it is possible to assume that Eu^{3+} ions entering in a 6*h* and 4*f* sites changes positions of ligands. The close microstructure of nearest oxygen environment of Eu^{3+} ions is formed. In work [17], the unique microstructure of a crystal field in "RE^{3+} ion+ligands" system was considered.

Some excitation spectra of the centers are given in Fig. 9. The spectrum of each center contains several narrow bands and one wide band. Peaks in the range 364–395 nm are caused by transitions $^7F_0 \rightarrow {}^5L_6$, $^5L_7$. Excitation wavelengths corresponding to these transitions have almost identical values for both centers. Wide bands are due to the transition to the charge transfer state. It is seen that the maximum values of the excitation wavelengths are different for both centers: λ_1=285 and λ_2=237 nm. This distinction of charge transfer band maximum wavelength occurs because nearest oxygen O^{2-} ions possess the different stability. Similar influence on a charge transfer band is described in [16]. Ion Eu^{3+} in a 4*f* site is surrounded by 9 oxygen ions belonging SiO_4. As to 6*h* position site Eu^{3+} ion is surrounded by 7 oxygen ions. And 6 of them belong SiO_4, the seventh called as "free" [18] locates into 2*a* position. Due to Y (Eu)–O bonds, RE^{3+} ions, being in 6*h* site, forms stable triangles oxygen tunnels (Fig. 2). "Free" oxygen ions can migrate in these tunnels [19,20].

The oxygen ions coordinating Eu^{3+} ions, are stabilized, mainly, by Si^{4+} ions. The oxygen ions stability, enclosing Eu^{3+} ions in a 4*f* site, is above, than in 6*h* site. It seems, "free" O^{2-} ion in a 2*a* site is less stabilized by surrounding positive ions, than other oxygen ions and consequently it is required to less energy for removal the electron from this ion [16].

The oxygen ions surrounding Eu^{3+} in the 6*h* position possess greater mobility than the europium environment in the 4*f* crystallographic position. Therefore it is possible to expect that the charge transfer band for the 6*h* position will be shifted to the long wavelength region of the spectrum. Note that these charge transfer bands have an ill-defined structure formed as a result of electronic-vibrational interactions of the charge transfer state with silicate lattice vibrations.

The excitation spectrum of $Sr_2Y_{6.8}Eu_{1.2}Si_6O_{26-\delta}$ shown in Fig. 10 was recorded at signals detected at various wavelengths. Wide bands in the range $\lambda_{ex}\sim 300-400$ nm (Fig. 10a) are caused by Eu^{2+} ion transition from the ground $4f^7$ ($^8S_{7/2}$) state to the excited $4f^65d$ state. There are sharp peaks on these bands. The first peak located at λ_{ex}=323 nm is likely to be due to absorption of radiation by oxygen vacancies, which ensure nonradiative transition of excitation energy to europium ions. Wide lines in the range λ_{ex}=260–360 nm are responsible for excitation of the charge transfer state in the two optical centers. It is noteworthy that Eu^{2+} excitation spectra and

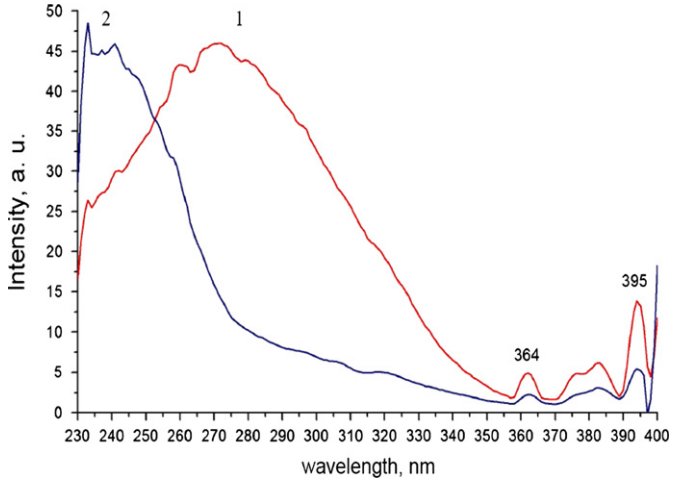

Fig. 9. Spectra of excitation of two optical centers generated Eu^{3+}: 1–λ_{em}=577, 2–581 nm.

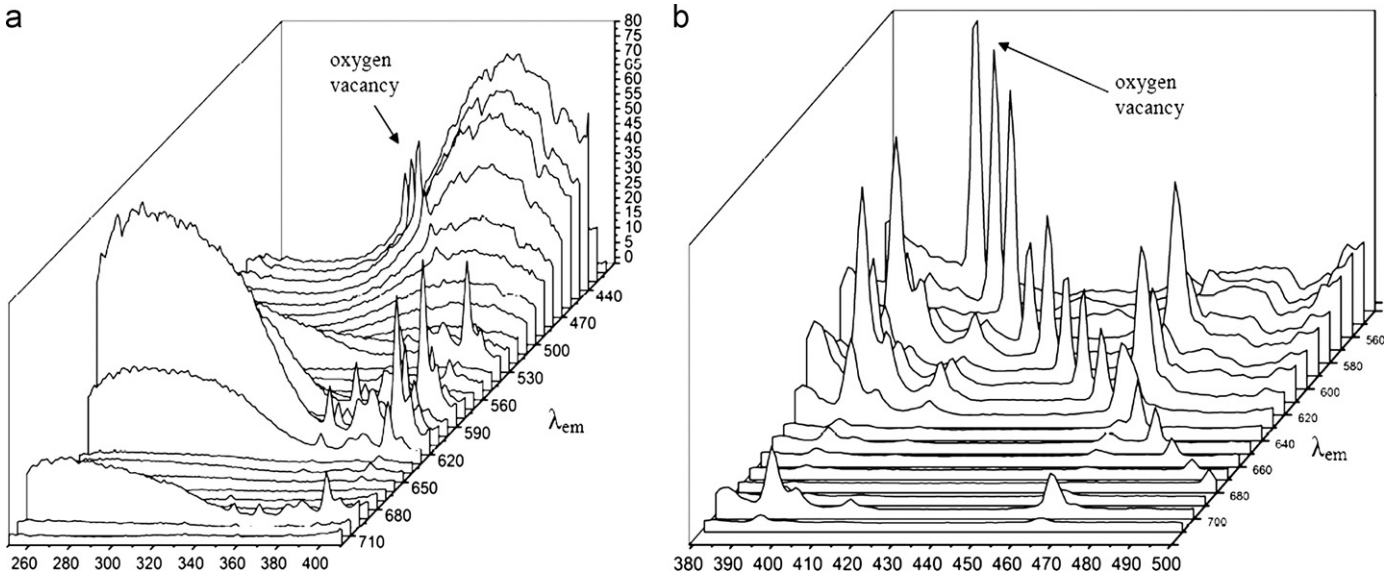

Fig. 10. Spectra of excitation of a luminescence of $Sr_2Y_{6.8}Eu_{1.2}Si_6O_{26-\delta}$, written down at detecting of signals on various of wavelength.

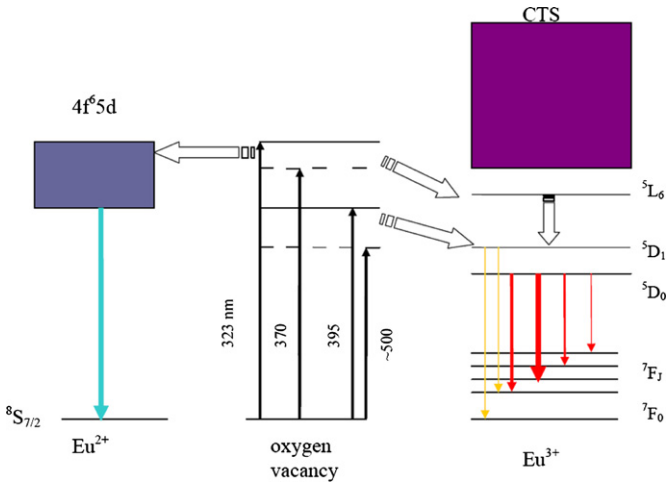

Fig. 11. The scheme of nonradiative transfer over of energy of excitation from oxygen vacancies to ions Eu^{2+} and Eu^{3+}.

charge transfer bands exhibit also a series of electron-vibrational transitions (Figs. 9 and 10). Fig. 10b displays a number of sharp peaks with decreasing intensity, which are also brought about by absorption of radiation by oxygen vacancies. As the wavelength of detected signals increases, the luminescence maxima of the peaks are displaced to the long-wave region of the spectrum. A similar displacement of lines in excitation spectra is described in work [21]. This displacement reflects an inhomogeneous character of oxygen vacancies distribution in the silicate matrix as in aluminum oxides [22].

On the basis of excitation spectra analysis, it is possible to allocate two states in electronic vacancies structure. The first is in an interval $\lambda_{ex} \sim 395-500$ nm, and the second is at $\lambda_{ex} \sim 323-370$ nm. As mentioned above at $x \leq 0.03$ the europium substitutes the yttrium in 6*h* site. In this case the Eu^{2+} ions can be formed in 6*h* site. Due to the vacancies occurs in short range ordering of Eu^{2+} ions. Hypothetically, the vacancies occur in 2*a* site. In addition this vacancy has inhomogeneous distribution. At $x > 0.03$ the mechanism of oxygen vacancies formation is similar.

Fig. 11 demonstrates a diagram of assumed nonradiative transfer of excitation energy from oxygen vacancies to Eu^{2+} and Eu^{3+} ions. Figured arrows indicate transfer to $4f^65d$ (Eu^{2+}) and $^5L_6$, $^5D_1$ (Eu^{3+}) states and between $^5L_6$ and $^5D_1$ states. Transitions induced by excitation of oxygen vacancies or by luminescence of Eu^{2+} and Eu^{3+} are denoted with ordinary arrows.

4. Conclusions

On the basis of analysis of spectral-luminescent characteristics of $Sr_2Y_{8(1-x)}Eu_{8x}Si_6O_{26-\delta}$ phosphors with the apatite structure it was established that Eu^{3+} ions form two types of optical centers. Besides, luminescence of Eu^{2+} ions was found. Reduction $Eu^{3+} \rightarrow Eu^{2+}$ in the crystals is caused by the formation of $V_{Sr}^{\parallel}$ vacancy in the 4*f* crystallographic position and by transfer of negative charge by this vacancy to two Eu_Y^{3+} ions. Thus, there exist oxygen-deficient centers, which are inhomogeneously distributed in the silicate lattice. As the wavelength of the detected signals increases, the luminescence maxima of the peaks are displaced to the long-wave region of the spectrum. The oxygen-deficient centers are responsible for nonradiative transfer of excitation energy to Eu^{3+} and Eu^{2+} ions. In the Eu^{2+} luminescence spectrum, a series of the lines is detected, which are due to the interaction of the $4f^65d$ state of Eu^{2+} ion with silicate lattice vibrations.

Acknowledgments

The authors are grateful to Dr. L.A. Perelyaeva and Dr. I.V. Baklanova for their assistance in recording IR and Raman spectra.

References

[1] C. Li, A. Lagriffoul, R. Moncorge, J.C. Souriau, C. Borel, Ch. Wyon, J. Lumin. 62 (1994) 157.
[2] RU Patent 2 186 162.
[3] RU Patent 2 379 328.
[4] M.D. Chambers, P.A. Rousseve, D.R. Clarke, J. Lumin. 129 (2009) 263.
[5] Nan Xiumei, Lin Jun, Li Zhe, QI Xiwei, LI Mingua, Wang Xiaoqiang, J. Rare Earths 26 (2008) 904.
[6] G. Seeta Rama Raju, Hong Chae Jung, Jin Young Park, Byung Kee Moon, R. Balakrishnaiah, Jung Hyun Jeong, Jung Hwan Kim, Sensors Actuators B 146 (2010) 395.
[7] Powder Diffraction File ICPDS—ICDD PDF2 (Relase 2005).
[8] Jun Ito, The Am. Miner. 53 (1968) 890.
[9] Inorganic Crystal Structure Database (ICSD) No. 155625.
[10] JunYang Cuimiao Zhang, Cuikun Lin, Chunxia Li, Jun Lin, J. Solid State Chem. 182 (2009) 1673.

[11] N. Lakshminarasimhan, U.V. Varadaraju, J. Solid State Chem. 178 (2005) 3284.
[12] L. Boyer, J. Carpena, J.L. Lacout, Solid State Ionics 95 (1997) 121.
[13] E.I. Getman, S.N. Loboda, T.V. Tkachenko, N.V. Yablochkova, K.A. Chebyshev, Russ. J. Inorg. Chem. 55 (2010) 333.
[14] V.G. Mazurenko, M.G. Zuev, Sov. Phys. Solid State 34 (1992) 1489.
[15] A. Orera, E. Kendrick, D.C. Apperley, V.M. Orera, P.R. Slater, Dalton Trans. (2008) 5296.
[16] G. Blasse, A. Bril, Philips Techn. Rev. 31 (1970) 304.
[17] Roger M. Macfarlane, J. Lumin. 100 (2002) 1.
[18] L. Boyer, B. Piriou, J. Carpena, J.L. Lacout, J. Alloys Compd. 311 (2000) 143.
[19] S. Lambert, A. Vincent, E. Bruneton, S. Beaudet-Savignat, F. Guillet, B. Minot, F. Bouree, J. Solid State Chem. 179 (2006) 2602.
[20] Julian R. Tolchard, M.Saiful Islam, Peter R. Slater, J. Mater. Chem. 13 (2003) 1956.
[21] G.S. Huang, X.L. Wu, Y.F. Mei, X.F. Shao, G.G. Siu, J. Appl. Phys. 93 (2003) 582.
[22] F.F. Komarov, A.V. Mudryi, L.A. Vlasukova, N.I. Mukhurov, A.V. Ivanyukovich, Opt. Spectr. 104 (2008) 235.